Indian Journal of Marine Sciences
Vol. 36(2), June 2007, pp. 141-151

Multifractal thermal characteristics of the western Philippine Sea upper layer

*Peter C. Chu & Chung-Ping Hsieh

Naval Ocean Analysis and Prediction Laboratory, Department of Oceanography, Naval Postgraduate School, Monterey, California 93943, USA

*[E-mail: pcchu@nps.edu]

Received 11 October 2006; revised 11 April 2007

Multifractal characteristics of the upper layer (above 140 m depth) thermal structure in the western Philippine Sea near Taiwan are analyzed using high-resolution, digital thermistor chain data. The power spectra at all the depths have multi-scale characteristics with the spectral exponent β in the range of (1, 2), which indicates nonstationary with stationary increments. The graph dimension varies from higher values such as 1.71 (in sublayer: 60 m), to lower values such as 1.59 (in second thermocline: 120 m). However, the information dimension varies slightly from 0.929 to 0.941. The multi-dimensional structure is stronger in nonstationarity (graph dimension) than in intermittency (information dimension). These results provide useful information for investigating turbulence structure in the upper layer of the western Philippine Sea.

[**Key words**: Multifractal structure, high-order structure function, singular measure, power law, multifractal plane]

1. Introduction

The western Philippine Sea (WPS) near eastern Taiwan (Fig. 1) is the region that the Philippines Current flows northward from just north of Mindanao (the southernmost of the main island groups of the Philippines) at around (10°N, 128°E) to Taiwan where it continues as the Kuroshio - the most evident western boundary current in the North Pacific Ocean. After becoming the Kuroshio, it makes a slight excursion into the South China Sea through the Luzon Strait, continues northward, and is fed from the North Equatorial Current, from which it continues to entrain water along its way. The Kuroshio current system has various stages of modification that transports warm water to the North Pacific. Because of the import and modification of water masses a large number of regional water types can be encountered.

Eddy activity is often observed in WPS near Taiwan. For example, a large warm eddy lies east of the Luzon Strait, a seemingly permanent feature[1-3]. Although the WPS is the only important source of open-ocean water to the South China Sea, the hydrographic and chemical properties of the waters on both side of the Luzon Strait are quite different[1]. Recent observations also show no evidence of branching of Kuroshio into the South China Sea, although Kuroshio water is often found inside the South China Sea[4]. It is likely that intrusion of the WPS water in the upper 600 m is caused by the (density) frontal instability of Kuroshio[5].

Oceanic density fronts often form cusp-like corrugation at the sea surface. These frontal cusps, ranging in scale from meters to kilometers, are often a prominent feature in radar images of coastal fronts. The complex three-dimensional flow structure underlying the surface cusp has been difficult to study despite many past observations. Two major features, nonstationarity and intermittency, should be first investigated in order to understand oceanic frontal instability. Question arises: How can we determine

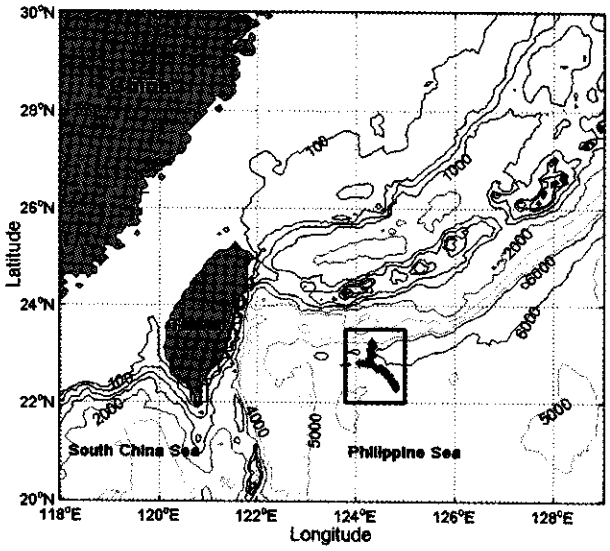

Fig. 1—Topography of the western Philippine Sea and surrounding areas. The inserted box shows the track of CMB.

Report Documentation Page

Form Approved
OMB No. 0704-0188

1. REPORT DATE	2. REPORT TYPE	3. DATES COVERED
2007		**00-00-2007 to 00-00-2007**

4. TITLE AND SUBTITLE	5a. CONTRACT NUMBER
Multifractal Thermal Characteristics of the Western Philippine Sea Upper Layer	5b. GRANT NUMBER
	5c. PROGRAM ELEMENT NUMBER
6. AUTHOR(S)	5d. PROJECT NUMBER
	5e. TASK NUMBER
	5f. WORK UNIT NUMBER
7. PERFORMING ORGANIZATION NAME(S) AND ADDRESS(ES) **Naval Postgraduate School,Department of Oceanography,Monterey,CA,93943**	8. PERFORMING ORGANIZATION REPORT NUMBER
9. SPONSORING/MONITORING AGENCY NAME(S) AND ADDRESS(ES)	10. SPONSOR/MONITOR'S ACRONYM(S)
	11. SPONSOR/MONITOR'S REPORT NUMBER(S)

12. DISTRIBUTION/AVAILABILITY STATEMENT
Approved for public release; distribution unlimited

13. SUPPLEMENTARY NOTES

14. ABSTRACT

15. SUBJECT TERMS

16. SECURITY CLASSIFICATION OF:			17. LIMITATION OF ABSTRACT	18. NUMBER OF PAGES	19a. NAME OF RESPONSIBLE PERSON
a. REPORT	b. ABSTRACT	c. THIS PAGE			
unclassified	**unclassified**	**unclassified**	**Same as Report (SAR)**	**11**	

upper ocean nonstationarity and intermittency from temperature observations? This paper uses a multifractal analysis on a high-resolution temperature dataset to obtain the nonstationarity and intermittency of the upper layer (140 m deep) in the WPS.

2. Coastal Monitoring Buoy with Attached Thermistors

The coastal monitoring buoy (CMB) was deployed by the U.S. Naval Oceanographic Office in WPS (Fig. 2) during 28 July – 7 August 2005. The original objective was to collect the data every 10 min near the air-sea interface. Above the ocean surface, the surface winds, air temperature, and air pressure were measured. Below the ocean surface, the temperature was observed at 1, 3, 5, 10, 15, and 20 m. Fifteen thermistors were attached to a wire rope extending from the code of CMB (20 m deep) to 140 m with high frequency sampling rate (every 15 sec) (Fig. 3). The purpose was to observe detail of the upper layer structure. Figure 4 shows contour plot of temperature ranging from 21°C to 29°C with 1.0°C increment on a vertical cross-section along the track (Fig. 2). The total length of the cross-section is 229.14 km. The CMB travels 3.82 m every 15 seconds.

The temperature shows a multi-scale variability with high irregularity. The surface mixed layer is very thin (depth around 5 m) on 28 July 2005 with temperature about 28.5 °C. Below the surface mixed layer, two thermoclines appear with the first thermocline to the depth of 50 m. The vertical gradient in the first thermocline is around 0.1°C/m. A relatively uniform sublayer (24 °C) exists below the first thermocline from 50 to 130 m. Below the uniform sublayer, there is a second thermocline with a vertical temperature gradient around 0.04 °C/m. As time approaches, the surface mixed layer deepens and the first thermocline descends. These processes

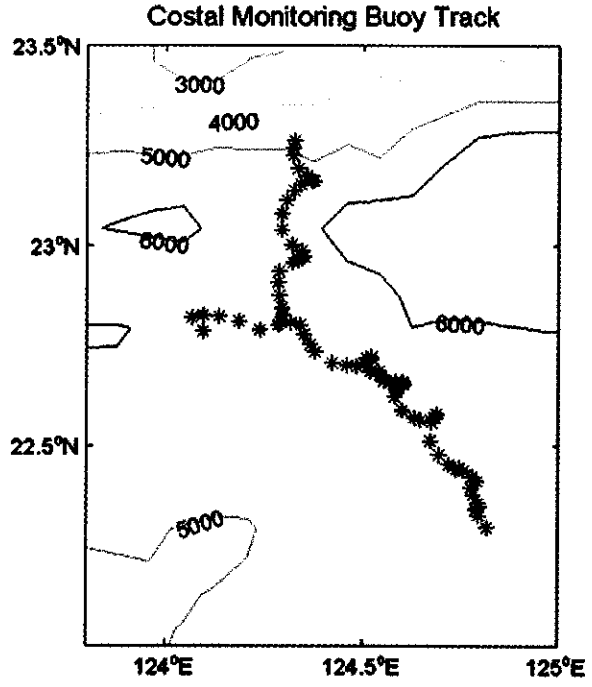

Fig. 2—Track of CMB (from July 28 to August 7, 2005) deployed by the Naval Oceanographic Office.

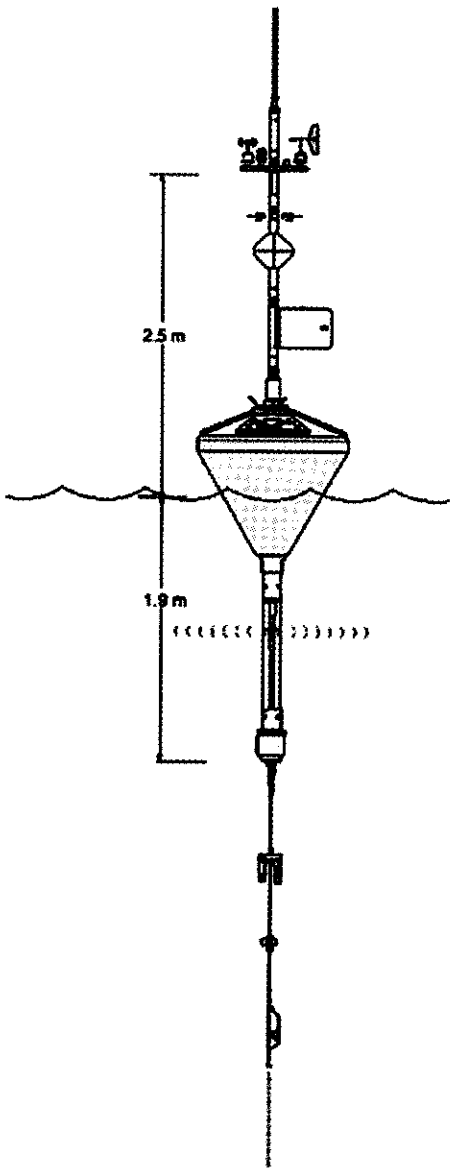

Fig. 3—The coastal monitoring buoy used in the WPS survey. Fifteen thermistors are attached to a wire rope extending from the code of CMB (20 m deep) to 140 m with high frequency sampling rate (every 15 sec).

contain small scale fluctuations. The surface mixed layer reaches 70 m on 5 August 2005, when an evident cooling occurs with the mixed layer temperature reducing to 25.5 °C. At the same time, the two thermoclines merge to a single themocline with the vertical gradient of 0.06 °C/m.

3. Power Spectra

Determination of the stationarity is the first step towards understanding the inherent thermal variability and statistical properties identified from this high-resolution temperature data with multi-layer structures. For a given depth, the temperature data is a function of the horizontal coordinates, x,

$$T_i = T(x_i),\ x_i = il,\ \ i = 0,1,...,\Lambda,\ \ \Lambda = L/l, \qquad \ldots (1)$$

where l = 3.8 m, is the horizontal resolution of the data, and L is the total horizontal scale of the data set. Our data set has 60,300 temperature profiles (Λ = 60,300).

Spectral analyses of temperature field,

$$E_j = E(k_j),\ \ k_j = j/L,\ \ j = 1,2,...,\Lambda/2 \qquad \ldots (2)$$

at all depths were conducted. Since large number of input values (60, 300) is considered, the Bartlett window is used after the Fast Fourier Transform in order to reduce the spectral leakage in the wavenumber domain. For the sake of brevity and to elucidate the important points, only spectra at six depths are shown in Fig. 5.

For a scaling process, one expects power law behavior[6,7],

$$E(k) \propto k^{-\beta}, \qquad \ldots (3)$$

over a large range of wavenumber k. The spectral exponent β contains information about the degree of stationarity of the data. If $\beta < 1$, the field is stationary; if $1 < \beta < 3$, the field contains nonstationary signal with stationary increments and in particular, the

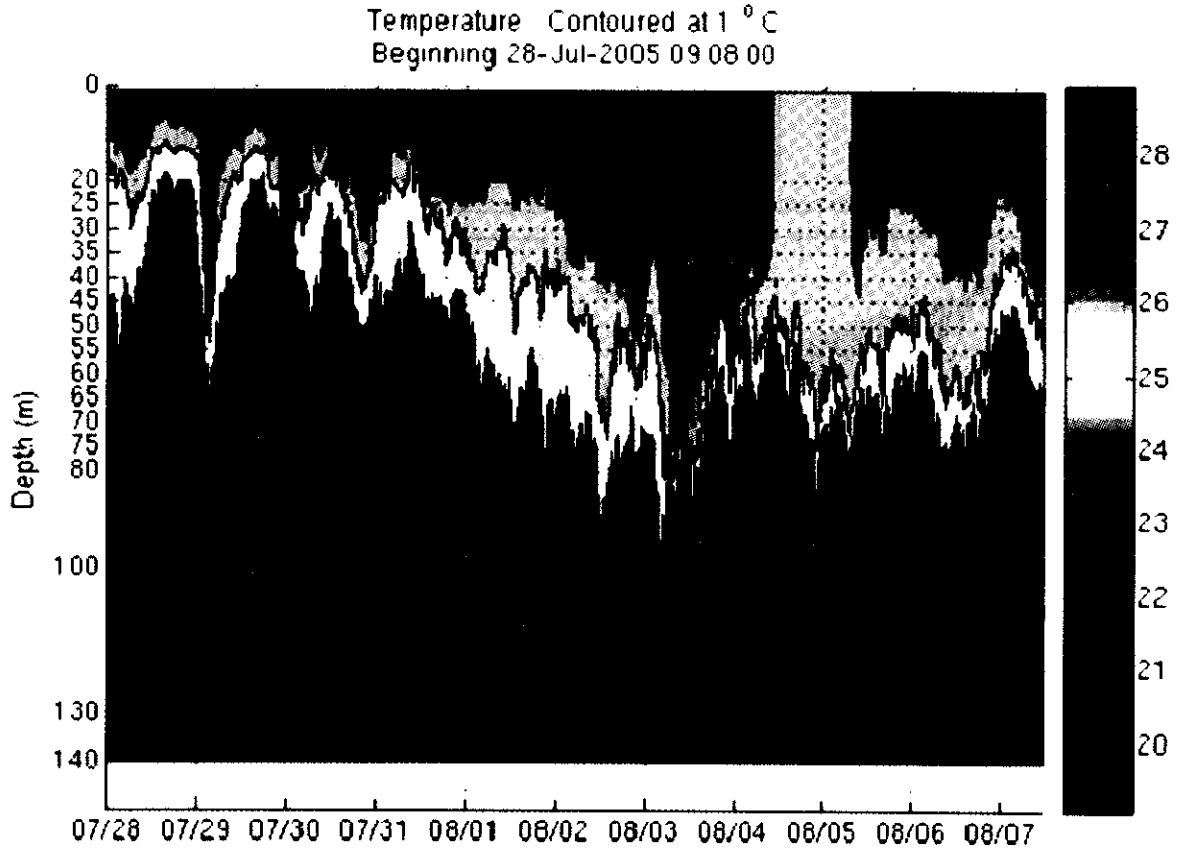

Fig. 4—Temperature cross section obtained from the CMB data collected along the track shown in Fig. 2.

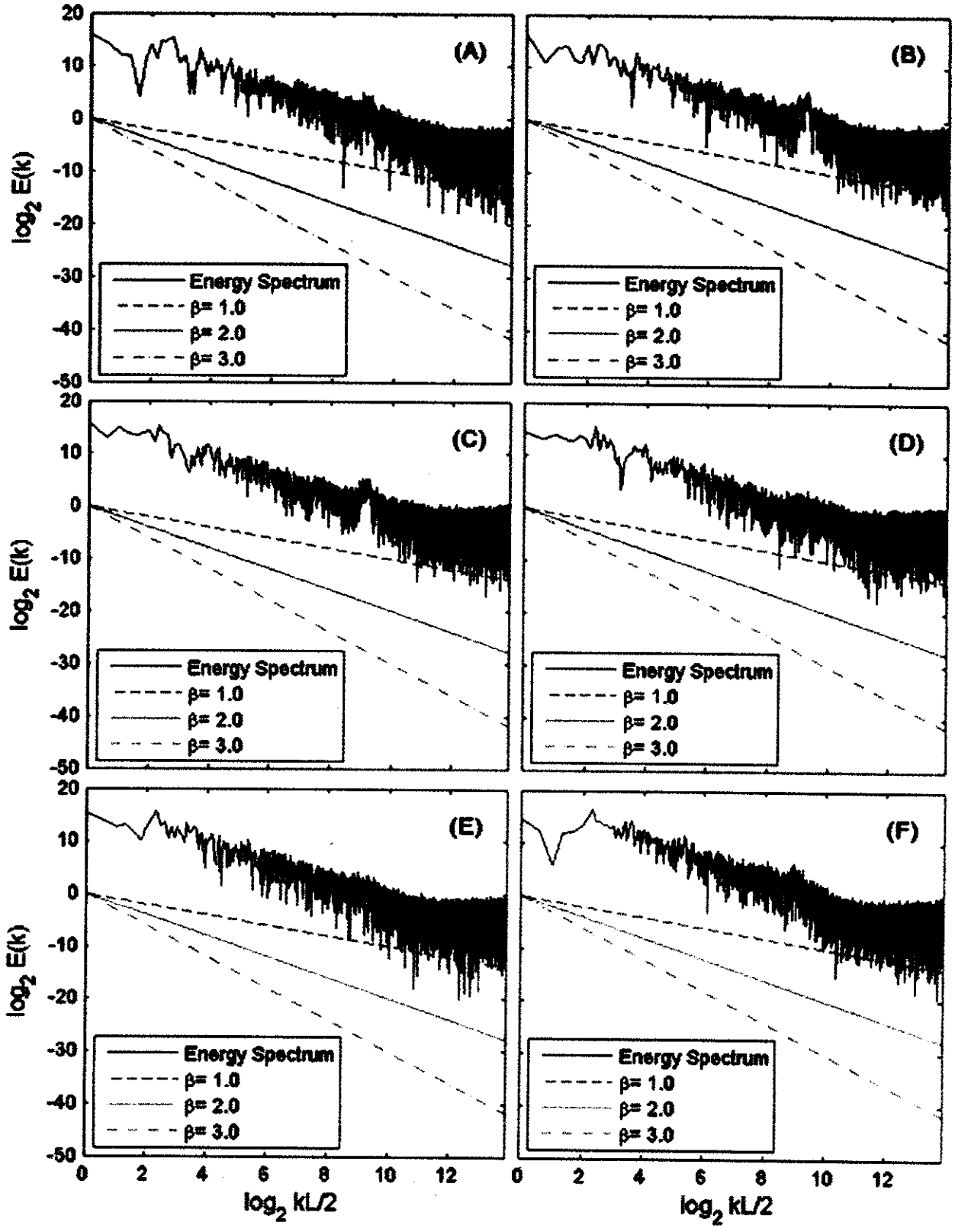

Fig. 5—Power spectra of temperature filed at depths of (A) 25 m, (B) 40 m, (C) 50 m, (D) 75 m, (E) 100 m, and (F) 140 m.

small-scale gradient field is stationary; if $\beta > 3$, the field is nonstationary with nonstationary increments. The power spectra for all the depths (Fig. 5) have multi-scale characteristics with the spectral exponent β in the range of

$$1 < \beta < 2, \quad \ldots (4)$$

which means the temperature field of the WPS upper layer is nonstationary with stationary increments.

4. Structure Functions

Since the thermistor chain data set has stationary increments, we should study the statistical characteristics of the gradient field,

$$|\Delta T(r;x)| = |T(x_{i+r}) - T(x_i)|, \quad i = 0,1,...,\Lambda - r, \ldots (5)$$

where r denotes the lag between two data points. The gradient may bound to create certain amount of noise and with different lags. However, the noise constitutes the high-frequency portion of the power law relation, it usually does not change the structure of the power law. Obviously, r is inversely proportional to the wavenumber k,

$$r \propto \frac{1}{k}.$$

Structure functions are used to depict the thermal variability. The qth-order structure function is defined by the mean of the q^{th} power of the gradient field $|\Delta T(r;x)|$,

$$S(r,q) \equiv \left\langle |\Delta T(r;x)|^q \right\rangle = \frac{1}{\Lambda - r} \sum_{i=0}^{\Lambda - r} |\Delta T(r;x)|^q. \quad \ldots (6)$$

For example, $r = 1$, $q = 1$, the structure function

$$S(1,1) = \frac{1}{\Lambda - 1} \sum_{i=0}^{\Lambda - 1} |T(x_{i+1}) - T(x_i)|, \quad \ldots (7)$$

represents the average magnitude of gradient.

Near-linear dependence of $\log_2[S(r,q)]$ on $\log_2(r)$ is found with different q-values from 0.5 to 4.0 (Fig. 6). The straight lines with different slopes show that the structure functions for the upper ocean temperature in the WPS satisfies the power law

$$S(r,q) \propto r^{\zeta(q)}, \quad \ldots (8)$$

with the exponent $\zeta(q)$ depending on q. Since S(r, 0) = 1, the power $\zeta(q)$ should be 0 for q = 0. Our computation (Fig. 6) agrees quite well with earlier studies in the southwestern Greenland Sea, Iceland Sea, and Norwegian Sea[6]: $\zeta(q)$ is monotonically and near-linearly increasing with q. Thus, it may be represented by

$$\zeta(q) = H(q)q, \quad \ldots (9)$$

where $H(q)$ is nearly a constant.

The power of the structure function, $\zeta(q)$, is computed for the whole dataset. Figure 7 shows the dependence of $\zeta(q)$ on q for selected levels. All the curves (near-linear) converges at q = 0 [$\zeta(0) = 0$], and show increase of $\zeta(q)$ with q for all depths. Such an increase is quite complicated as $q < 3$ and shows three different patterns as $q > 3$: (a) slow increasing with q in the sub-layer (50 – 80 m), (b) intermediate-rate increasing with q in the upper thermocline (35 – 45 m) and lower thermocline (100 - 140 m), (c) fast increasing with q in the mixed layer (25 - 30 m).

The structure function for q = 1, $S(r, 1)$, is often used to determine the statistical characteristics of the data such as stochastically continuous and stationarity. When the structure function $S(r, 1)$ does not depend on r

$$S(r,1) = \text{const}, \quad \ldots (10)$$

which denotes exact stationary. Eq. (10) is equivalent to

$$\zeta(1) = H(1) = 0.$$

Thus, $H_1 \equiv H(1)$, represents statistical characteristics of data. Since the power $\zeta(1)$ [i.e., $H(1)$] varies with depth (Fig. 7) between 0.29 at 60 m depth (sub-layer) and 0.41 at 140 m depth (second thermocline), the thermal field in the WPS is nearly stationary.

If $g(T)$ is defined as the graph of $T(x)$, whose dimension can be defined[8] by

$$D_{g(T)} = 2 - H_1. \quad \ldots (11)$$

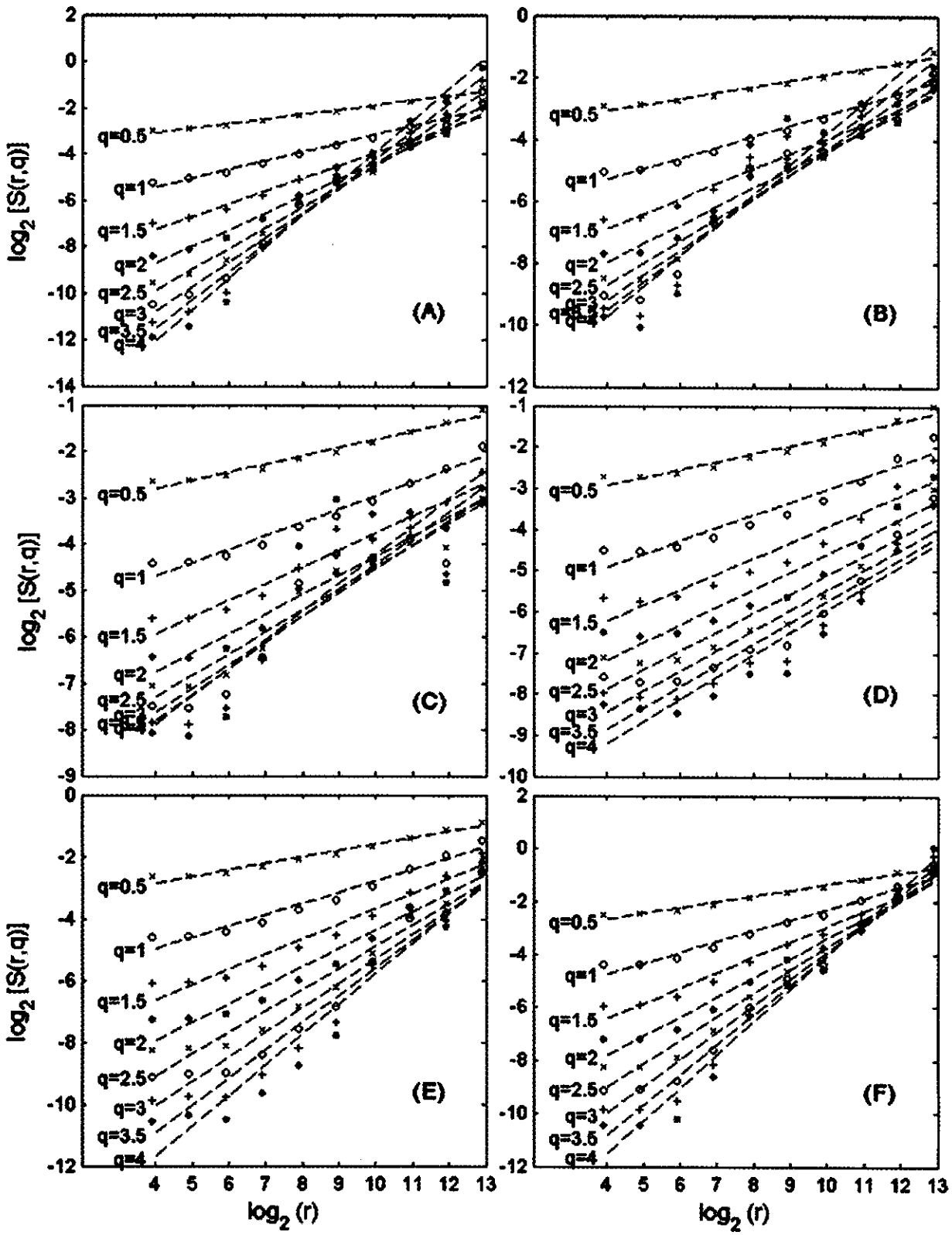

Fig. 6—Structure functions for different q-values at depths of (A) 25 m, (B) 40 m, (C) 50 m, (D) 75 m, (E) 100 m, and (F) 140 m.

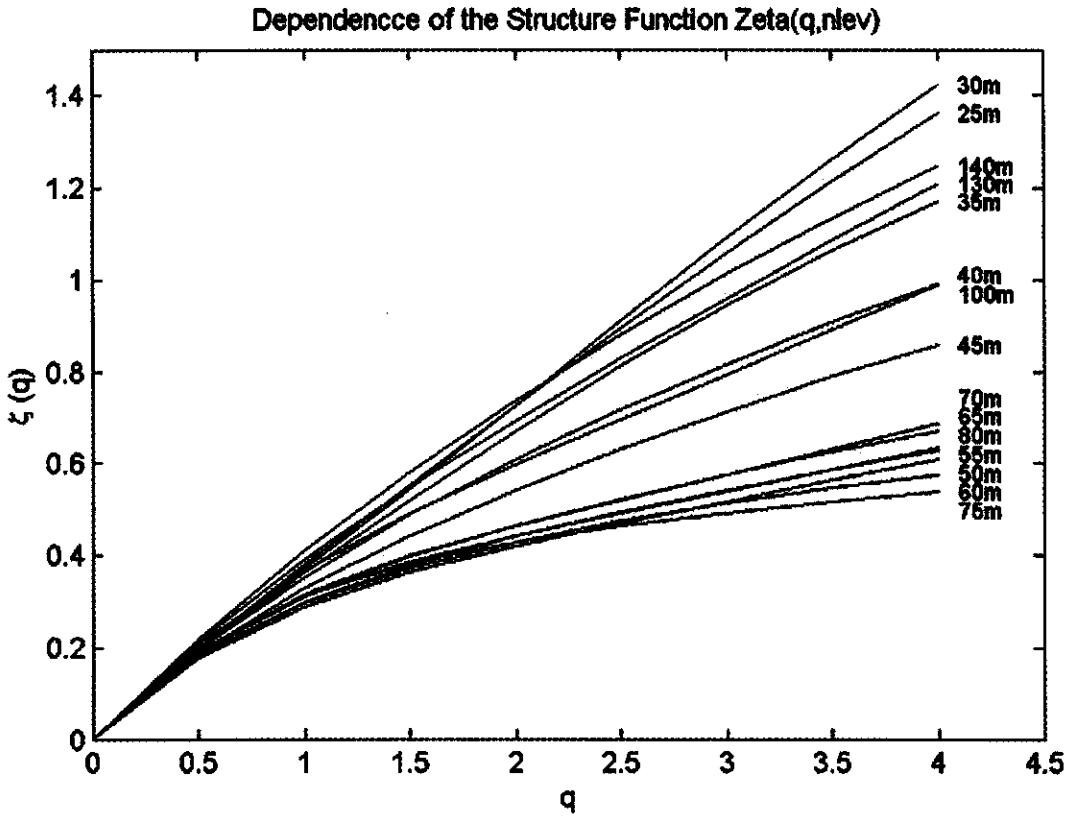

Fig. 7—Dependence of the structure function's power, $\zeta(q)$, on q and depth.

For a stochastically continuous ($H_1 = 1$) data $T(x)$, the graph is a smooth curve, whose dimension, $D_{g(T)} = 1$. If the graphs $g(T)$ fill the whole space (exact stationary),

$$D_{g(T)} = 2, \qquad \ldots (12)$$

which corresponds to $H_1 = 0$. The graph dimension of upper thermal field of the WPS varies (multi-dimension structure) from higher values such as 1.71 (sublayer: 60 m), to lower values such as 1.59 (second thermocline: 120 m).

5. Singular Measures

Normalized small scale absolute gradient

$$\varepsilon(1;x_i) = \frac{|\Delta T(1;x_i)|}{\left\langle |\Delta T(1;x_i)| \right\rangle}, \qquad \ldots (13)$$

$$\left\langle |\Delta T(1;x_i)| \right\rangle = \frac{1}{\Lambda}\sum_{i=0}^{\Lambda-1} |\Delta T(1;x_i)|,$$

is used to identify the intermittency of the thermal field. The running average of r normalized values are computed by

$$\varepsilon(r;x_i) = \frac{1}{r}\sum_{j=i}^{i+r-1} \varepsilon(1;x_j), \quad i = 0,1,\ldots,\Lambda - r. \qquad \ldots (14)$$

The mean of the qth power of $\varepsilon(r;x_i)$

$$M(r,q) \equiv \left\langle \varepsilon(r;x_i)^q \right\rangle = \frac{1}{\Lambda - r}\sum_{i=0}^{\Lambda-r} [\varepsilon(r;x_i)]^q, \qquad \ldots (15)$$

is defined as the qth-order singular measure. Obviously, for $q = 0$,

$$M(r, 0) = 1. \qquad \ldots (16)$$

For $q = 1$,

$$M(r,1) \equiv \left\langle \varepsilon(r;x_i) \right\rangle = \frac{1}{\Lambda - r}\sum_{i=0}^{\Lambda-r} [\varepsilon(r;x_i)]$$

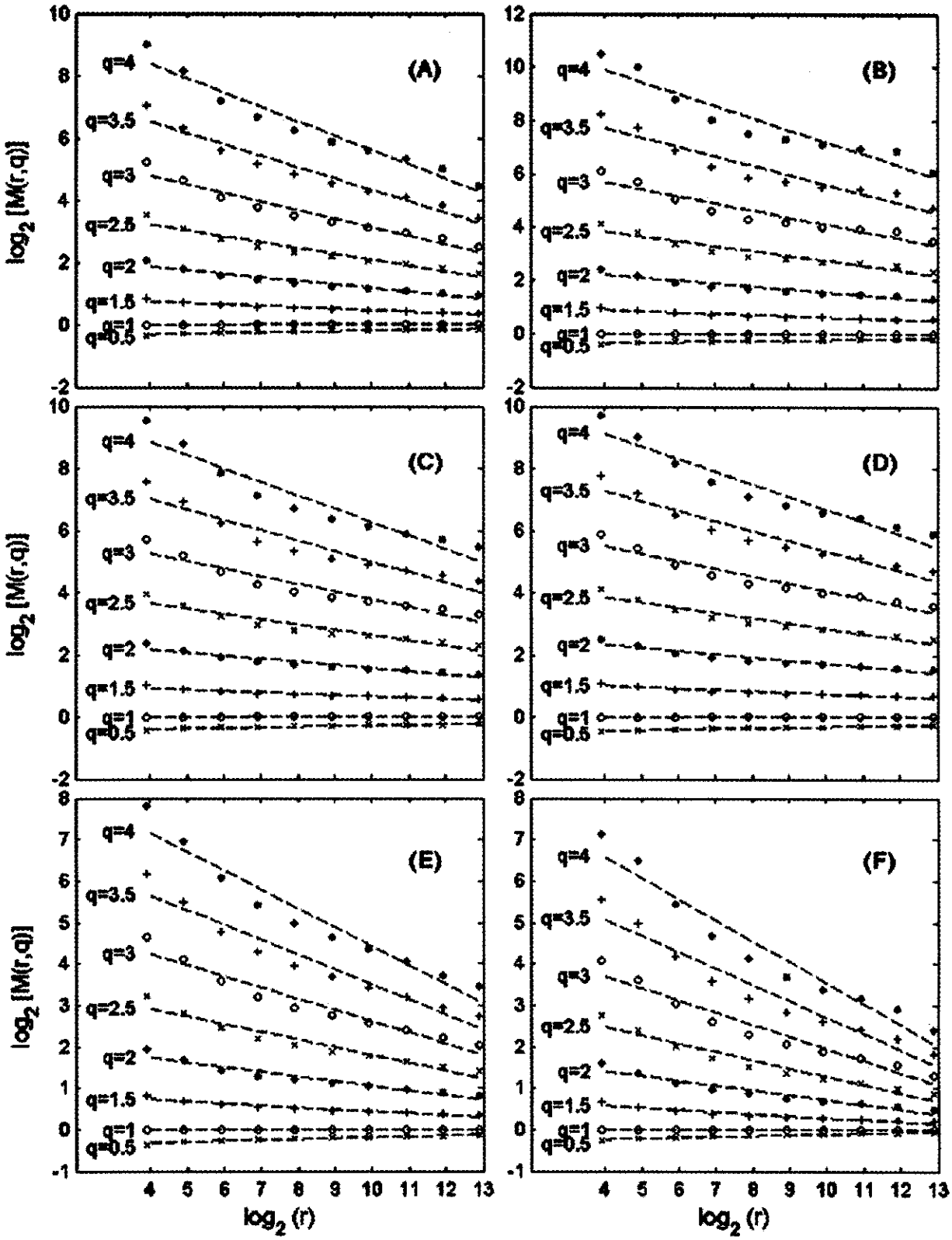

Fig. 8—Singular measures for different q-values at depths of (A) 25 m, Bb) 40 m, (C) 50 m, (D) 75 m, (E) 100 m, and (F) 140 m.

$$= \frac{1}{\Lambda - r} \sum_{i=0}^{\Lambda - r} \left[\frac{1}{r} \sum_{j=i}^{i+r-1} \varepsilon(1; x_j) \right] = 1. \quad \ldots (17)$$

The singular measures are computed for all depths. For simplicity, $M(r, q)$ for six depths (25, 40, 50, 75, 100, 140 m) is given here (Fig. 8). Near-linear dependence of $\log_2[M(r,q)]$ on $\log_2(r)$ is found with different q-values from 0.5 to 4.0. The straight lines with different slopes show that the singular measures with various q for the upper layer temperature in the WPS satisfies the power law

$$M(r,q) \propto r^{-K(q)}, \quad q \geq 0, \quad \ldots (18)$$

with the power $K(q)$ varying with q. From Eqs. (16) and (17), we have

$$K(0) = K(1) = 0. \quad \ldots (19)$$

Several characteristics are found from Fig. 9: The power $K(q)$ is a convex function

$$\frac{d^2K(q)}{dq^2} > 0, \quad \ldots (20)$$

for all q and

$$K(q) < 0 \quad \text{only if} \quad 0 < q < 1 \quad \ldots (21)$$

which reflects the fact that, in this range, taking a q^{th} power necessarily reduces the fluctuation of $\varepsilon(r; x_i)$; and otherwise

$$K(q) \geq 0, \quad \text{if} \quad q \geq 0. \quad \ldots (22)$$

Following Chu[6], we may define a function

$$C(q) = \frac{K(q)}{q-1}. \quad \ldots (23)$$

For $q \to 1$, we use *l'Hospital*'s rule to define a straightforward measure of inhomogeneity in the sense of singular measure

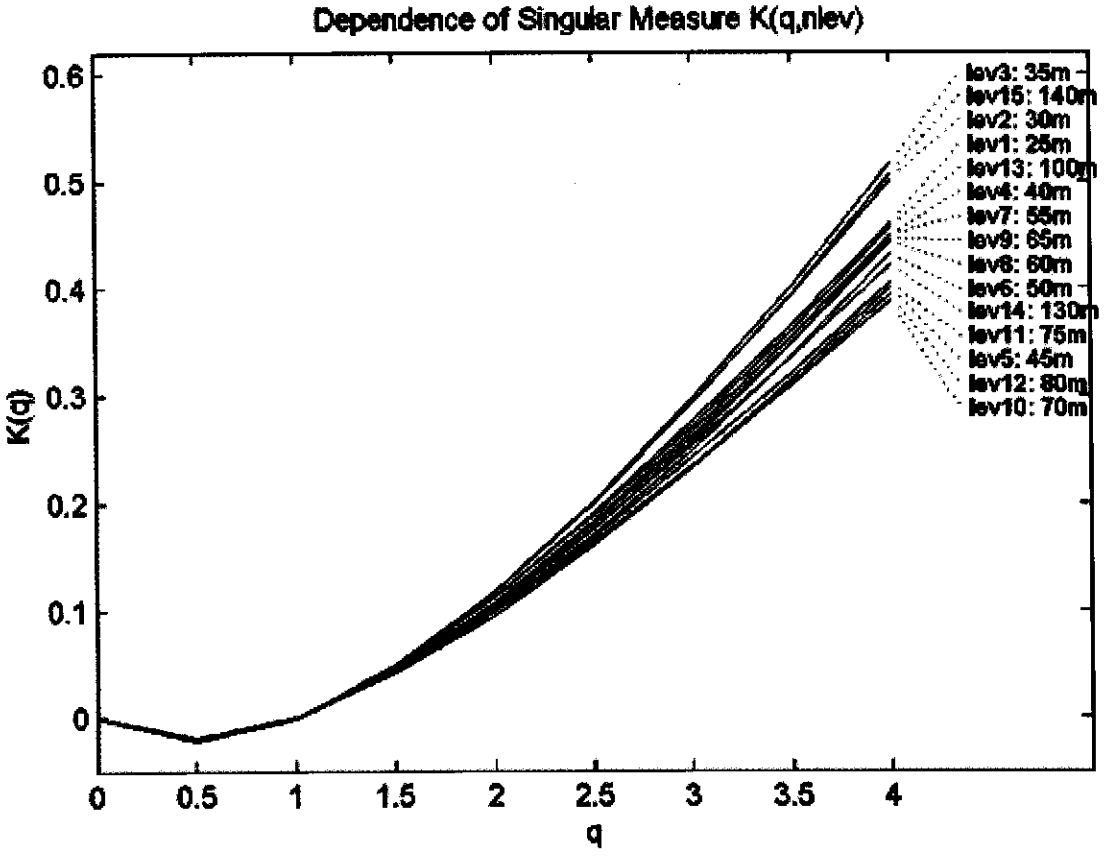

Fig. 9—Dependence of the singular measure's power, $K(q)$, on q and depth.

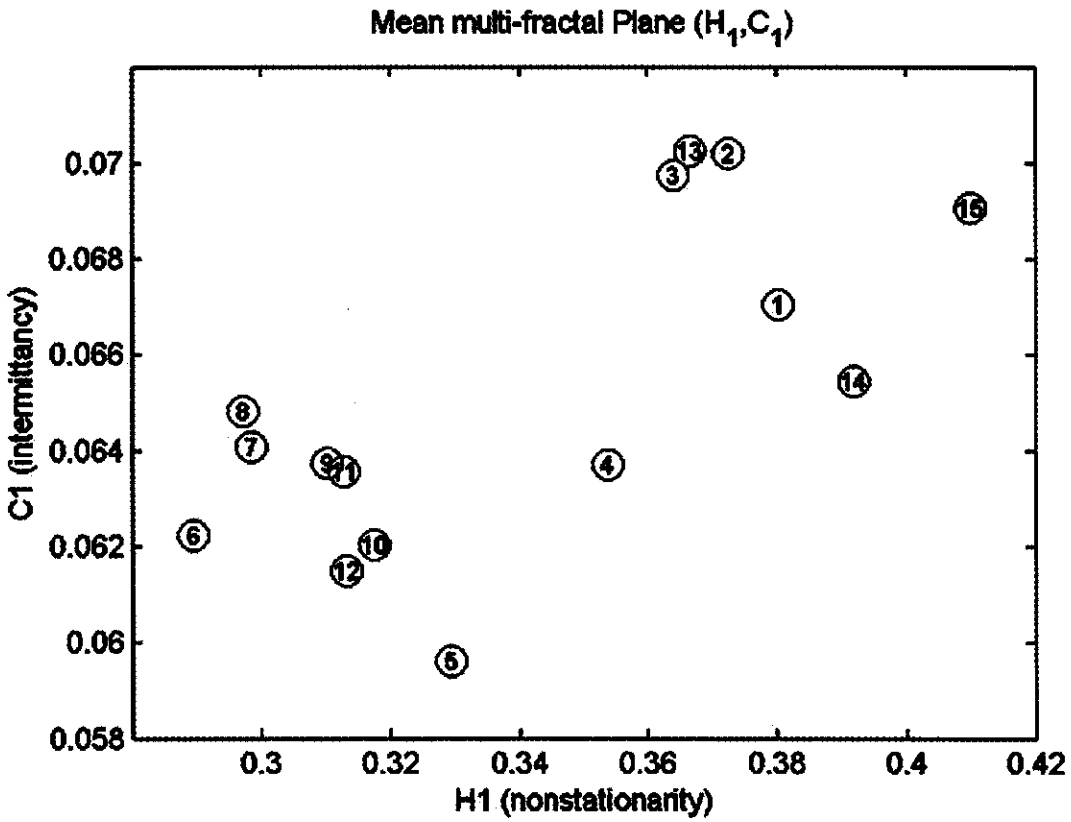

Fig. 10—Mean multi-fractal plane (H_1, C_1) for the western Philippine Sea thermal field.

$$C_1 \equiv C(1) = K'(1) \geq 0, \quad \ldots (24)$$

which is called the intermittency parameter. The larger the value of C_1, the lager the intermittency and singularity the data set has. The intermittency parameter C_1 varies from 0.059 to 0.071.

6. Mean Multifractal Plane

Statistical moments of all orders (qth power) can be computed, however, the first moment ($q = 1$) provides important information about the data. Roughness indicates differentiability while singularity indicates uniqueness. Sparseness may be inferred as either lack of information or no continuity, but it does not mean singularity. Roughness constitutes with information and shows continuity and for that reason it can be differentiable. The parameter C_1 measures the degree of intermittency in the system, while H_1 measures its degree of nonstationarity.

The plot of C_1 versus H_1, called the mean multifractal plane, shows the degree of nonstaionarity and intermittency (Fig. 10). Both parameters have geometrical interpretations as co-dimensions: information dimension and graph dimension[6]. The information dimension, represented by (1 - C_1), is a first-order estimate of sparseness of strong gradient distributed in the system. The graph dimension, represented by (2 - H_1), is a first-order estimate of roughness in the system. Both parameters have analytical meanings: C_1 (sparseness) is related to singularity and H_1 (roughness) is connected to the lack of differentiability. The WPS upper layer thermal field shows multifractal characteristics (Fig. 10) in terms of C_1 and H_1. We find larger variation in H_1 (0.29-0.41) than in C_1 (0.059-0.071). Identification of (H_1, C_1) ranges helps to select realistic model to describe the field.

7. Conclusion

The upper layer thermal structure in the western Philippine Sea has the following multifractal features:

(1) The power spectra at all the depths have multi-scale characteristics with the spectral exponent β in the range of (1, 2). This means the temperature field is nonstationary with stationary increments.

(2) The structure function has multifractal characteristics. The powers of the qth-order structure function show three different patterns: (a) slow increasing with q in the sub-layer (50 – 80 m), (b) intermediate-rate increasing with q in the upper thermocline (35 – 45 m) and lower thermocline (100 - 140 m), (c) fast increasing with q in the mixed layer (25 - 30 m).

(3) Two parameters for the first moment (q = 1) structure function and sigular measure, H_1 and C_1, are important to represent the multifractal characteristics in terms of co-dimensions (information and graph). The graph dimension, represented by (2 - H_1), is a first-order estimate of roughness in the system. The information dimension, represented by (1 - C_1), is a first-order estimate of sparseness of strong gradient distributed in the system. Both parameters have analytical meanings: C_1 (sparseness) is related to singularity and H_1 (roughness) is connected to the lack of differentiability.

The graph dimension of the upper thermal field of the western Philippine Sea varies (multi-dimension structure) from higher values such as 1.71 (sublayer: 60 m), to lower values such as 1.59 (second thermocline: 120 m). However, the information dimension of the western Philippine Sea upper thermal field varies slightly from 0.929 to 0.941. This indicates that singularity is very low.

8. Acknowledgement

This work was funded by the Office of Naval Research, Naval Oceanographic Office, and the Naval Postgraduate School.

9. References

1 Nitani, H., Beginning of Kuroshio. In *Kuroshio: Its physical aspects*, edited by H. Stommel and K. Yoshida, (University of Tokyo Press, Tokyo), 1972, pp. 129-163.

2 Chu, P.C., & Li, R.F., South China Sea isopycnal surface circulation, *J. Phys. Oceanogr.*, 30, (2000), 2419-2438.

3 Chu, P.C., & Fan, C.W., Low salinity, cool-core cyclonic eddy detected northwest of Luzonduring the South China Sea Monsoon Experiment (SCSMEX) in July 1998, *J. Ocenogr.*, 57, (2001), 549-563.

4 Xu, J.P., & Su, J.L., Hydrographic analysis on the intrusion of the Kuroshio into the South China Sea, Part 2, Observational results during the cruise from August to September in 1994, *Tropic Oceanol.*, 16, (1997), 1-23 (in Chinese).

5 Su, J.L., & Lobanov, V.B., Eastern Asia, Kamchatka to the eastern coast of the Philippines coastal section (10, w), In *The sea*, Vol 11, *The global coastal ocean*, edited by A. R. Robinson and K. H. Brink, (John Wiley and Sons, Inc., New York), 1998, pp. 415-427.

6 Chu, P.C., Multifractal thermal characteristics of the southwestern GIN Sea upper layer, *Chaos, Solitons & Fractals*, 19, (2004), 275-284.

7 Chu, P.C., Ivanov, L.M., Kantha, L., Melnichenko, O., & Poberezhny, Y., Power law decay in model predictability skill, *Geophys. Res. Lett.*, 29, (2002), 10.1029/2002 GLO14891.

8 Mandelbrot, B.B., *The fractal geometry of nature*, (W. H. Freeman, New York), 1982, pp. 460.